Analysis of End Loss and Optimization of Critical Compensation Dimensions for a Non-Tracking Parabolic Trough Concentrator

Tianfang Zhao
School of Energy and Environmental Science, Yunnan Normal University, Kunming , China
Xu Ji
School of Energy and Environmental Science,
Yunnan Normal University, Kunming , China
Bianfeng Yang
School of Physics and Electronic Information,
Yunnan Normal University, Kunming , China

Introduction

The parabolic trough collector (PTC) is a representative system for solar concentrating utilization. Its optical efficiency is influenced not only by mirror reflectivity, receiver transmittance, absorptance, and intercept factor [1,2], but also closely related to end loss [3].

Regarding end loss, Xu et al. [4] derived an analytical expression for the end-loss ratio of a horizontal north–south-axis PTC and proposed an end-plane mirror compensation method. Li et al. [5] further established a general end-loss model for PTCs with arbitrary orientation and proposed compensation strategies such as extending the absorber tube, installing fan-shaped end-plane mirrors, and tilting the collector.

Although previous studies have developed end-loss models for arbitrarily oriented PTCs and proposed various compensation methods, research remains limited on end loss in east–west arranged non-tracking PTCs caused by changes in the solar east/west position, as well as its matching relationship with receiver and reflector lengths. In this study, the Zemax ray-tracing method is used to systematically analyze the influence of incidence angle on the end-loss ratio of PTCs. By comparing two compensation strategies—extending the receiver length and shortening the reflector length—the critical compensation dimensions required to achieve zero end loss at different incidence angles are determined.

End-Loss Mechanism of PTC and Zemax Ray-Tracing

MECHANISM OF END LOSS AND SYSTEM STRUCTURE

Due to the apparent motion of the sun across the sky, sunlight cannot always be incident perpendicularly on the collector aperture. When there is a certain angle between the incident rays and the collector, rays striking the edge of the parabolic surface are reflected and then undergo an axial displacement by the time they reach the focal line, making them unable to be intercepted by the receiver and resulting in end loss, as shown in Fig. 1. The structure of this concentrator and the related geometric relationships of the transverse angle and longitudinal angle are shown in Fig. 2. By fixing the transverse angle (θ) at 0° and varying the longitudinal incidence angle (α), the effect of the sun's east–west positional change on end loss is analyzed.

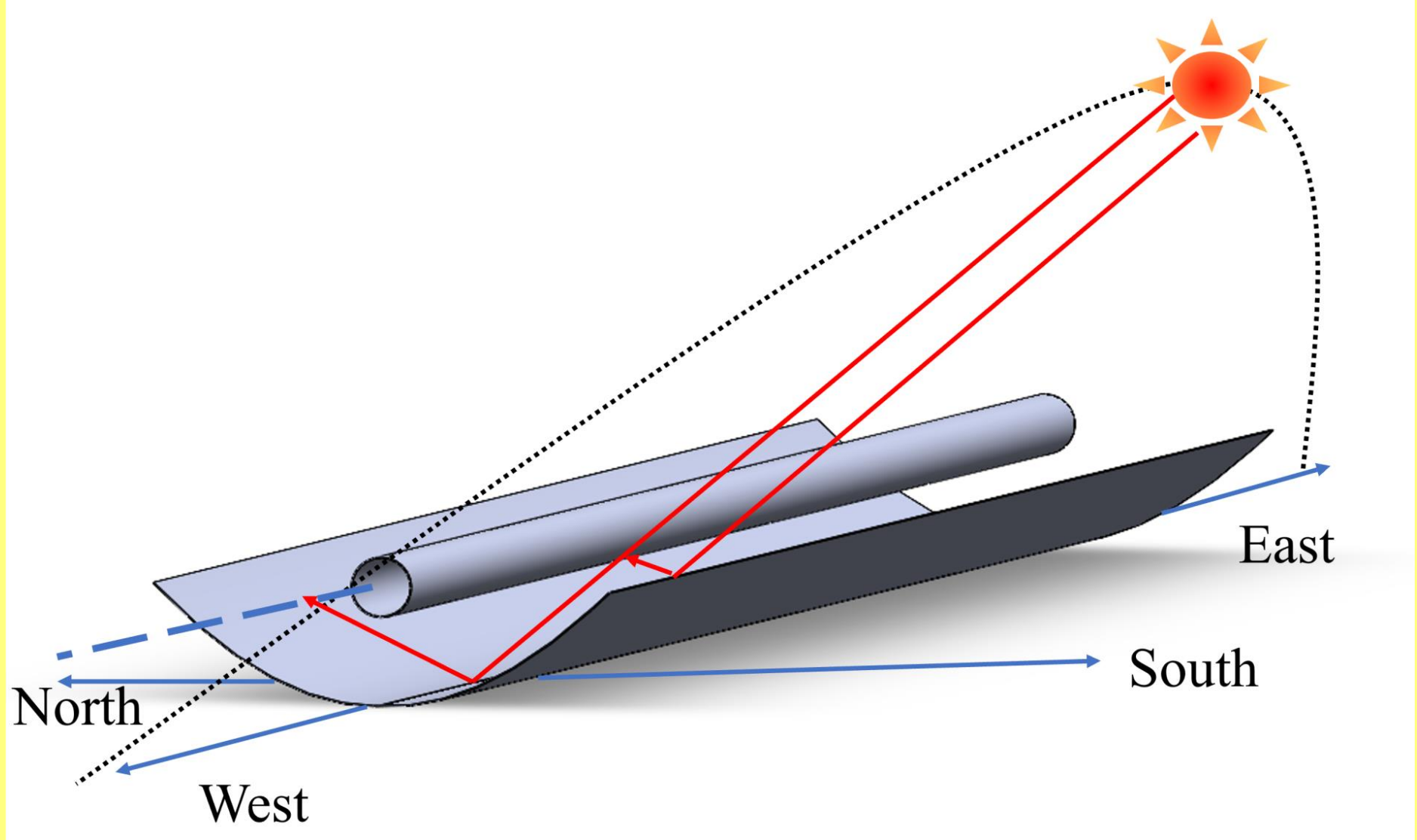

Fig.1. Schematic diagram of end loss in PTC.

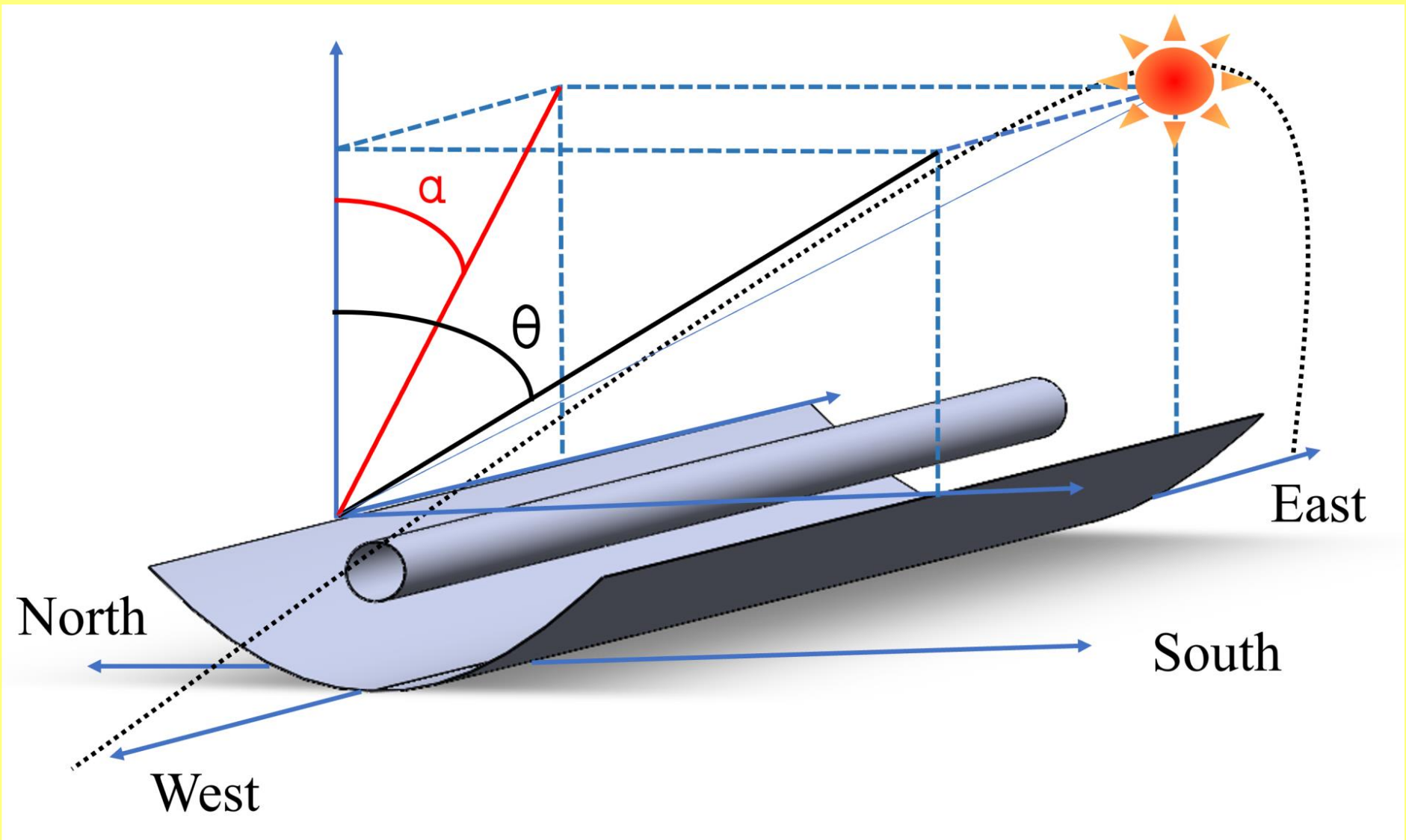

Fig. 2. Horizontal schematic diagram of non-tracking parabolic trough concentrator.

RAY-TRACING SETUP AND SIMULATION CONDITIONS

To highlight end loss caused by changes in the sun's east–west position, no additional transverse off-axis angle was introduced in the ray-tracing simulations, ensuring that the focusing state in the cross-sectional plane remained unaffected. In addition, a sufficiently large number of traced rays (about 20,000) was used for all cases to reduce statistical fluctuations and ensure result convergence.

This study used Zemax to analyze the effects of three different conditions on the end-loss behavior of the PTC. Details are as follows:

The first category is the equal-length condition for the receiver and reflector, where the receiver length is kept equal to the reflector length (1.8 m). Under this condition, the influence of longitudinal incidence angle on the end-loss rate is investigated. The longitudinal incidence angle range analyzed is 0°–20° (with a 1° step), with additional cases at 30° and 40°. This condition is used to reveal the basic variation pattern of end loss in an equal-length configuration and to serve as the baseline for subsequent compensation conditions.

The second category is the receiver-extension compensation condition. At selected longitudinal incidence angles, the reflector length is kept constant, and the variation of end-loss rate with different receiver extension lengths is analyzed. This condition is used to determine the minimum receiver extension required to reduce end loss to zero at a given longitudinal incidence angle.

The third category is the reflector-shortening compensation condition. At the same longitudinal incidence angles as in the second category, the receiver length is kept constant, and the variation of end-loss rate with reflector shortening is analyzed. It is then used to determine the minimum reflector shortening required to achieve zero end loss.

Results

VARIATION PATTERN OF END-LOSS RATE UNDER THE EQUAL-LENGTH CONDITION

With the receiver and reflector configured to have equal lengths, the end-loss ratio shows a significant positive correlation with the longitudinal incidence angle. As the longitudinal incidence angle increases from 0° to 40°, the end-loss ratio exhibits an almost linear upward trend. At a longitudinal incidence angle of 20°, the end-loss ratio reaches about 33.15%; when the angle further increases to 40°, the loss ratio rises markedly to about 76.18%, as shown in Fig 3.

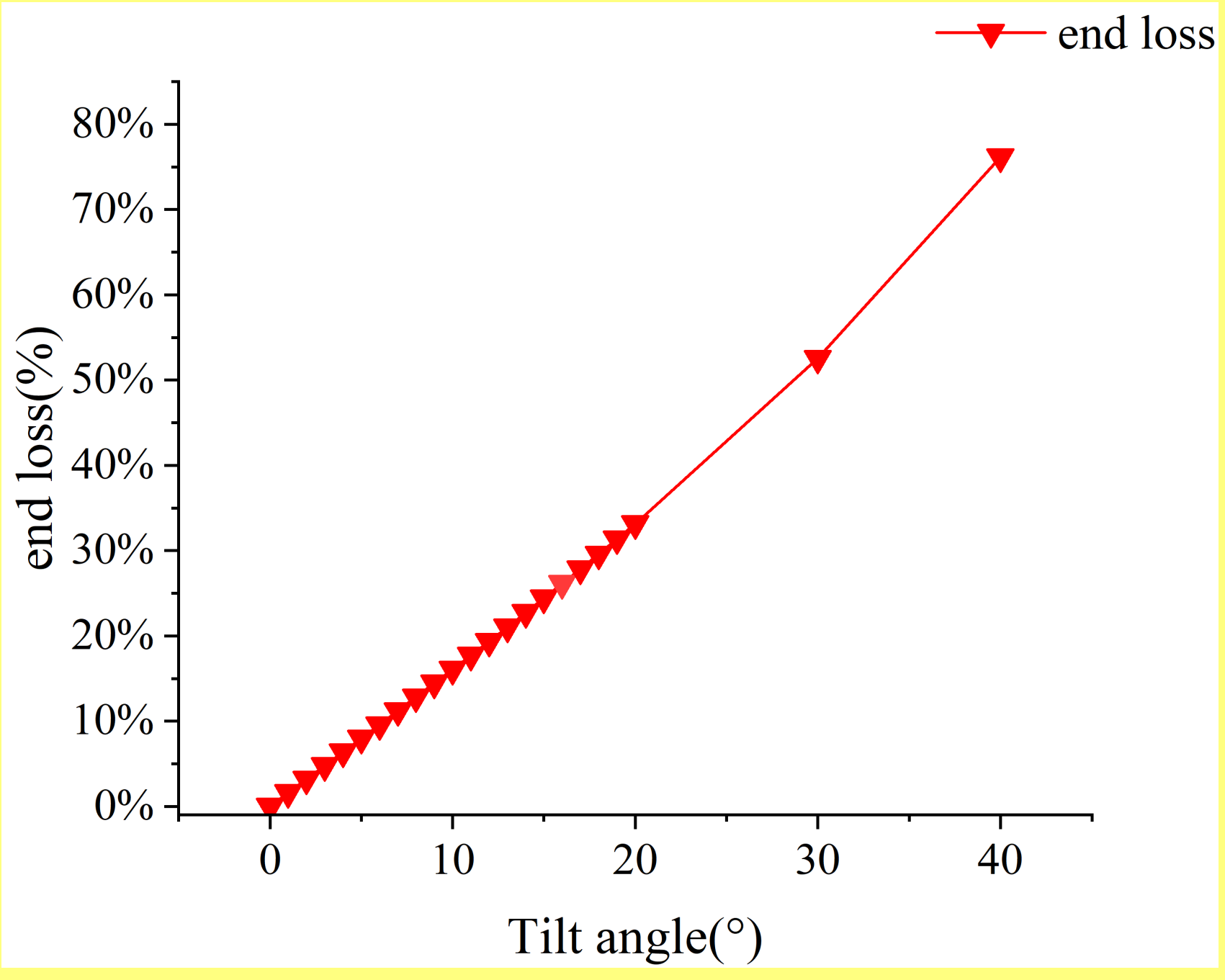

Fig. 3. Variation of the end loss rate with α when both reflector and receiver are 1.8 m in length.

COMPENSATION EFFECTS OF INCREASING RECEIVER LENGTH AND SHORTENING THE REFLECTOR

Increasing the receiver length and shortening the reflector length are direct approaches to compensate for end loss. Fig. 4a summarizes the total one-side receiver extension required to achieve zero end loss, and Fig. 4b summarizes the total one-side reflector shortening required to achieve zero end loss at different longitudinal incidence angles. Both compensation dimensions show a very strong linear positive correlation with the longitudinal incidence angle.

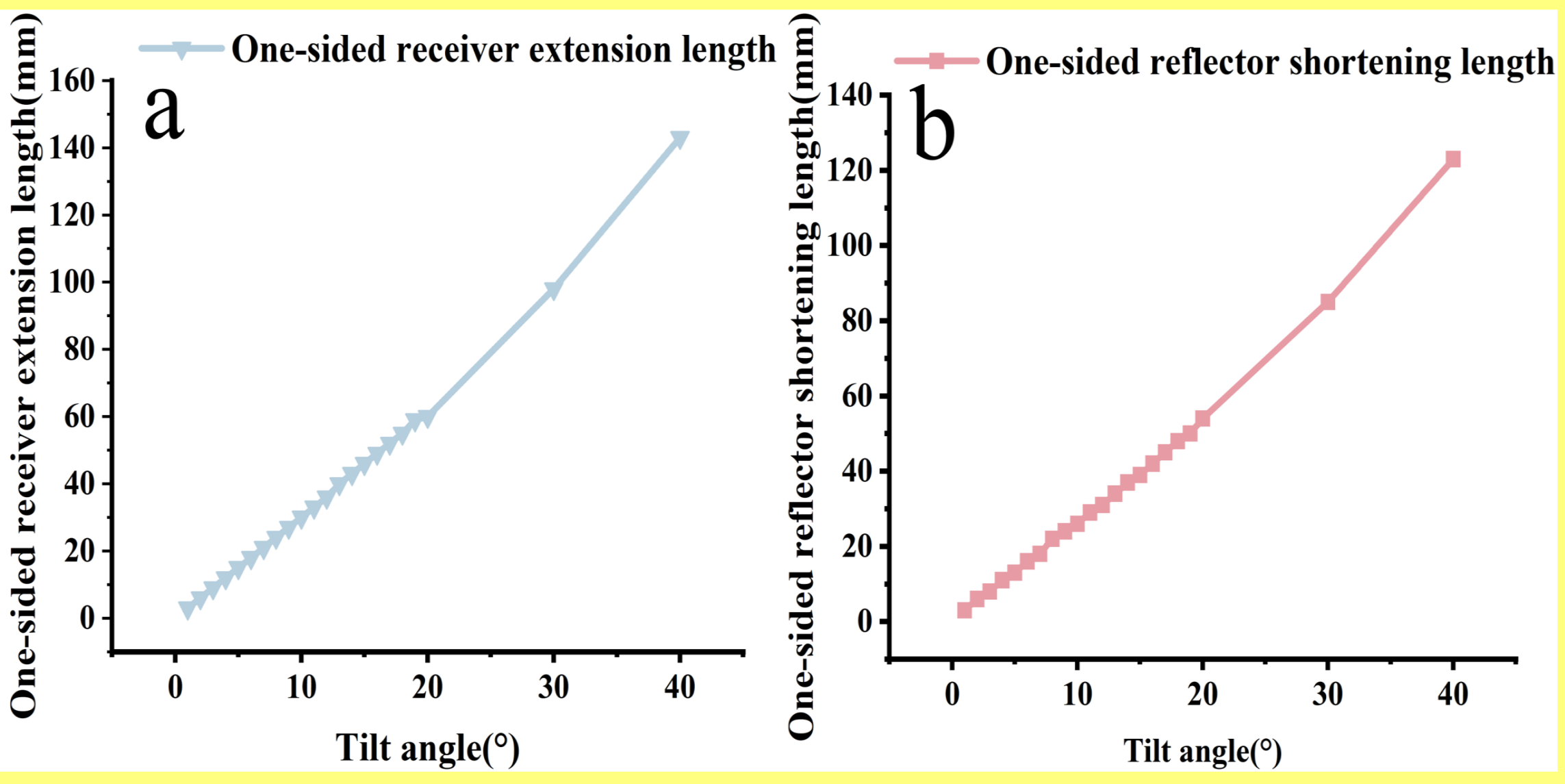

Fig. 4. (a) One-sided receiver extension required to achieve zero end loss at different α;(b) One-sided reflector shortening length required to achieve zero end loss at different α.

COMPARISON OF TWO COMPENSATION STRATEGIES

Fig 5 presents a comparison of the two compensation strategies, with the y-axis representing the normalized compensation length, defined as the ratio of the one-side compensation amount to the original baseline length. From the perspective of eliminating end loss, both methods can reduce the end-loss ratio to zero at specific tilt angles; however, they differ fundamentally in implementation approach and design cost.

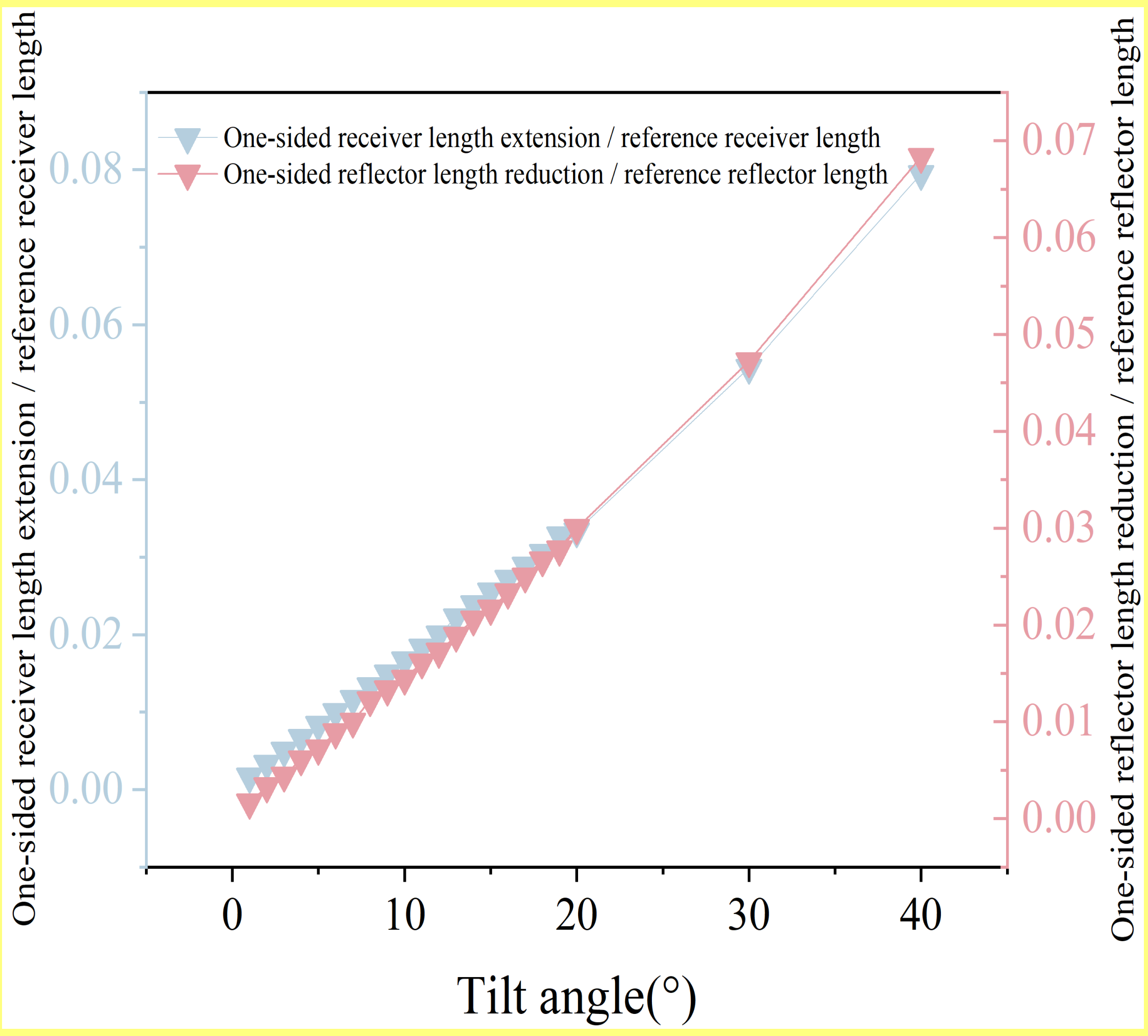

Fig. 5. Comparison of two compensation strategies.

Conclusions

Under the equal-length condition of the receiver and reflector, the end-loss rate increases significantly with increasing longitudinal incidence angle. As the longitudinal incidence angle increases from 0° to 20°, the end-loss rate rises from 0 to 33.15%.

Both compensation strategies—extending the receiver and shortening the reflector—can achieve a zero end-loss rate at specific tilt angles; however, they differ fundamentally in implementation approach and design cost.

Both the required one-side receiver extension length and the required one-side reflector shortening length exhibit a very strong positive linear correlation with the longitudinal incidence angle.

References

[1] Reddy K S, Ajay C S, Nitin Kumar B. Sensitivity study of thermal performance characteristics based on optical parameters for direct steam generation in parabolic trough collectors [J]. Solar Energy, 2018, 169: 577-593.

[2] Fuqiang W, Ziming C, Jianyu T, et al. Progress in concentrated solar power technology with parabolic trough collector system: A comprehensive review [J]. Renewable and Sustainable Energy Reviews, 2017, 79: 1314-1328.

[3] Sandá A, Moya S L, Valenzuela L. Modelling and simulation tools for direct steam generation in parabolic-trough solar collectors: A review [J]. Renewable and Sustainable Energy Reviews, 2019, 113: 109226.

[4] Xu C, Chen Z, Li M, et al. Research on the compensation of the end loss effect for parabolic trough solar collectors [J]. Applied Energy, 2014, 115: 128-139.

[5] Li M, Xu C, Ji X, et al. A new study on the end loss effect for parabolic trough solar collectors [J]. Energy, 2015, 82: 382-394.